IFSCC 2025 full paper (IFSCC2025-1504)

Achieving Flawless Skin: Advancements in Pore Analysis with AI and Computer Vision Technologies.

Cristina Bonell [1], Haohan Peng [2], Belen Aguirre [1], Mauricio Valerio-Santiago [1], Gemma Mola [1] and Raquel Delgado [1]

[1] Lubrizol Life Science, Lipotec S.A.U., Barcelona, Spain.
[2] Lubrizol, Corporate Technology, Pudong, China.

1. Introduction

The cosmetic industry has evolved significantly, moving beyond merely addressing traditional signs of facial aging, such as wrinkles and spots. Today, the emphasis is on promoting healthy aging with skin that is free from impurities and visibly smooth. This shift has led to a growing consumer interest in the detailed examination of various skin features, with a particular focus on visible pores [1].

Pore visibility affects both female and male subjects and is influenced by a range of factors. Overactive sebaceous glands in oily skin types, acne changes throughout life, and the natural loss of skin elasticity and increased sagging due to aging contribute to enlarged and more visible pores [2,3]. These changes can affect the overall appearance of the skin, making it appear less smooth and more textured.

Traditional methods of pore analysis have primarily relied on subjective manual quantification, leading to inconsistencies in results. This approach is not only time-consuming but also limited in its scope, often failing to capture the full complexity of pore features. In recent years, commercial software for image analysis has improved, making the evaluation of facial pores easier. However, most existing technologies may not yet handle the details required for an in-depth evaluation, nor provide comprehensive, accurate, and exceptionally fast analysis of their features. These limitations in quantifying complex pore parameters underscore the need for more advanced solutions. To address this, we have developed novel image-processing methodologies that leverage advancements in computer vision and artificial intelligence (AI).

First, we created a methodology by using trained algorithms to automatically identify the region of interest (ROI) in images where pores are more pronounced: the cheek areas from both lateral and frontal facial images. By generating masks through a multi-step process, pores are detected for further analysis of their features.

Second, we developed two methodologies designed for pore analysis from high-resolution 3D images obtained from two commercial devices. One device can create a mask with detected pores on the overall facial image, showing their depth with a color scale. Utilizing computer vision capabilities, we can extract several quantifiable parameters, providing more detailed

information. The other device provides more objective information, such as number, depth, and circularity of pores from a section of the face. Using the obtained images with highlighted pores, we have focused on a more in-depth analysis of age-related visible pores, which tend to be not only enlarged but also more elongated.

2. Materials and Methods

2.1. Automated pore detection from 2D facial images

The initial phase in developing the pore detection application involved creating a database of images and masks for training the algorithm. The database consisted of 2D RGB facial images from frontal and 45-degree perspectives (Nikon D7200). Two different approaches were employed to crop the cheeks as the regions of interest (ROIs).

For the 45-degree images, we developed an interactive code that displayed the image to the user, who then defined four points to outline the ROI. These points were used to crop the image, saving the resulting ROI as a new image.

For the frontal images, we utilized the MediaPipe Python library [4]. MediaPipe is a powerful open-source library that provides efficient machine learning solutions for real-time applications, such as face detection. The selected MediaPipe code detects the entire human face and generates corresponding landmarks or reference points in real-time. In 2D space, the left and right cheek regions were defined based on these landmarks. The extracted landmark points were then smoothed using cubic spline interpolation [5] to create refined and continuous cheek contours. Subsequently, the largest inscribed rectangle within the smoothed contour was identified, ensuring that only the cheek regions were selected. The resulting rectangles served as the ROIs and were automatically cropped and saved as new images.

After creating all the ROIs, the next step was generating the masks. The masks creation process consisted of multiple steps, starting with frequency filtering. The frequency filtering process removes background noise, thereby isolating and enhancing salient information in the images. Low frequencies in an image refer to gradual changes in color or intensity, such as large areas of shadow or smooth transitions, commonly found in regions like cavities or deep wrinkles. In contrast, high frequencies represent rapid and sharp variations in color or intensity, highlighting edges and fine details like pores. In essence, low frequencies capture large and soft features, while high frequencies focus on small and intricate details.

The filtered images underwent histogram equalization to enhance contrast, making features more distinguishable [6]. After equalization, K-means clustering was applied to identify the darkest grayscale values, which served as a threshold to create a binary mask, highlighting regions associated with low frequencies likely to be pores [7]. The mask was further refined by detecting and filtering contours based on their shape and size, isolating the relevant features. This process resulted in the creation of a final, refined mask. Figure 1 shows an example of the image reference and the generated mask.

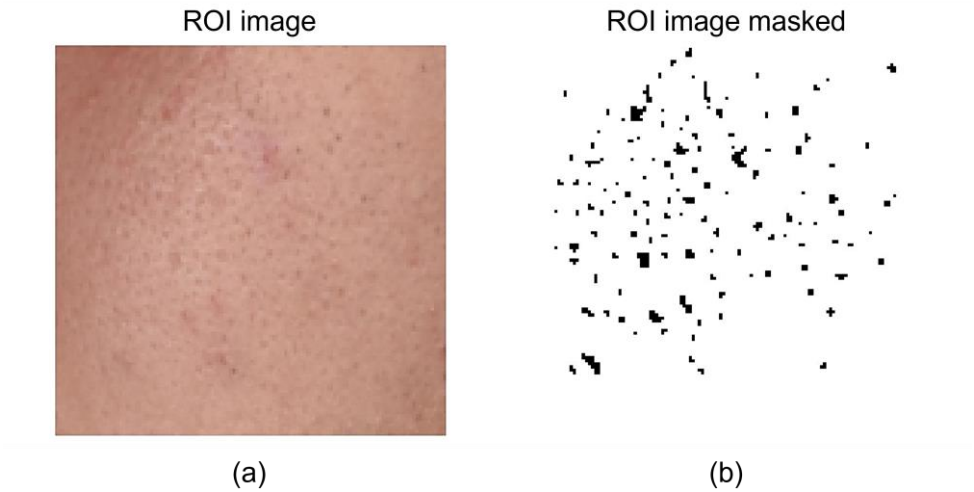

Figure 1. Image example of pores detection process: (a) Image of ROI obtained check area; (b) Mask of pores created by the model.

Once ROIs and masks were created for training, the model was designed using a classical neural network architecture [8], which enhances the accuracy of details. It was combined with a robust backbone for image processing to boost the model's efficiency in patterns recognition [8,9].

The model was developed through three distinct stages. During the training phase, which served as the instructional period, we used a total of 187 images. In the validation phase, designed to verify the training results, 51 images were included. After the model was considered trained, we proceeded to the testing phase, where 56 images were assessed to conduct a final evaluation of the model's performance.

Data augmentation was performed over the three sets to increase the amount of data available. The chosen augmentations were subtle, involving slight adjustments to brightness, color, and contrast, along with horizontal flipping and small rotations of up to 5 degrees.

2.2. Pore Depth Classification Method from 3D Images

There are 3D imaging devices available on the market capable of capturing detailed images of the skin's surface. However, some do not provide quantified information directly from these images. The application we developed can extract several quantifiable parameters, offering more detailed information about facial pores.

The 3D images of cheek pores, which included a color scale map to indicate depth, were acquired from a commercial device (LifeViz® Infinity, QuantifiCare). By employing K-means clustering, we quantified several 2D parameters and classified the pores according to their depth by analyzing the pixel colors. The process started by establishing reference points based on skin tone and the color map, followed by background removal and the creation of a pore mask. The analysis focused on specific target colors, such as yellow and the volunteer's skin tone, along with colors representing depth progression of pores from smallest to greatest: orange, green, blue, and purple. Areas identified as yellow were excluded as their characteristics did not qualify them as notably visible pores. Scheme 1 shows the workflow of the filter application process on the original image.

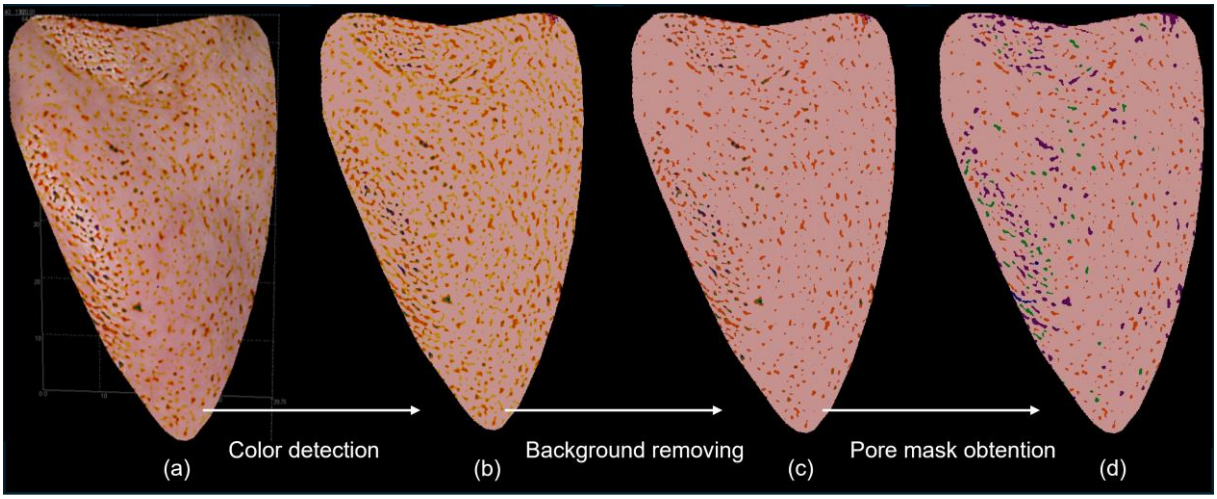

Scheme 1. Representation of the algorithm process flow: (a) Input image of cheek area from LifeViz® Infinity; (b) Color detection by K-means algorithm; (c) Yellow and skin tone section removed; (d) Colors merged based on depth: orange, green, blue and purple.

Using the remaining four colors from the processed images, we accurately counted the number of pores, measured their size and density, determined the distribution of pores across different depth levels, and calculated the average pore size and pore depth.

2.3. Deepening the Evaluation of Age-Related Pores

Other software of commercial devices provides numerical data about pore characteristics such as size, number, and depth. Nevertheless, for assessing the anti-aging efficacy of cosmetic ingredients, our interest lies specifically in elongated pores, as they are associated with the skin aging process.

To evaluate the features of these specific elongated pores, computer vision techniques were implemented. For each subject, the device's software (Antera 3D®, Miravex) generates two images that highlighted the pores and displayed a color map indicating their depth: one displaying all pores and the other focusing exclusively on circular pores. A dataset comprising these types of images from the cheek area was collected. Then, an initial approximation of elongated pores was obtained by isolating them through the subtraction of the circular pore map from the map of all pores, using a script specifically developed for this purpose. From the resulting images, a secondary filtering process using K-means clustering algorithm was conducted. By fitting an ellipse around each pore to fully enclose it, the area and the elongation ratio were determined. This approach allowed a precise extraction of actual enlarged and elongated pores. This second step was essential because the non-circular pores identified in the previous subtraction do not specifically correspond to elongated pores; the image also contained very small pores and pores with edges or other non-elongated shapes.

After successfully extracting the desired pores, several parameters were calculated, including the number of pores, their area and length, their depth as indicated by the color map, and the elongation ratio.

Scheme 2 illustrates the workflow of the image processing, starting from the original image of the device to the final image of age-related pores mask.

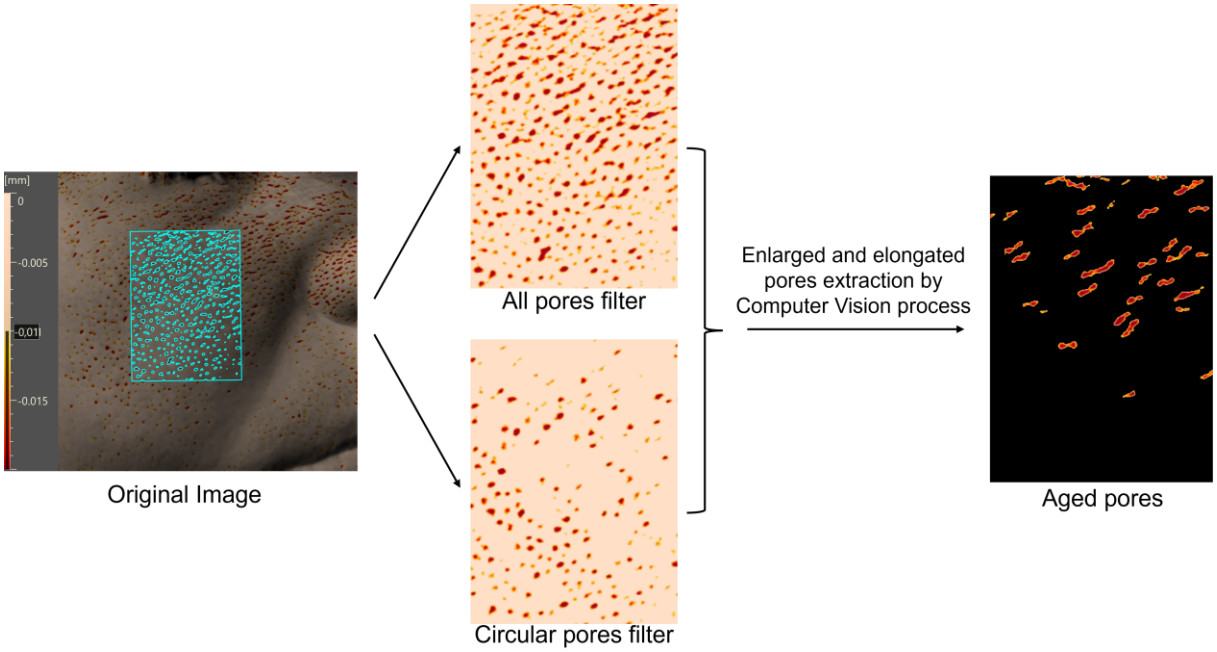

Scheme 2. Overview of image processing for age-related pores obtention from Antera 3D® device images.

3. Results

3.1. Performance Assessment of Pore Detection Tool

To evaluate the performance of the pore detection model, the Intersection over Union (IoU) metric was selected [10]. IoU measures the ratio of the intersection to the union of the predicted and actual reference masks; it is 1 when the prediction perfectly matches the mask and 0 when there is no overlap. The IoU between the reference and the prediction during the training stage was approximately 0.94, which is considered a strong indicator of the performance model. Figure 2 illustrates two examples of processed images. The original image, the reference, and the prediction, visually demonstrate that the model effectively manages the pore detection of the cheek area.

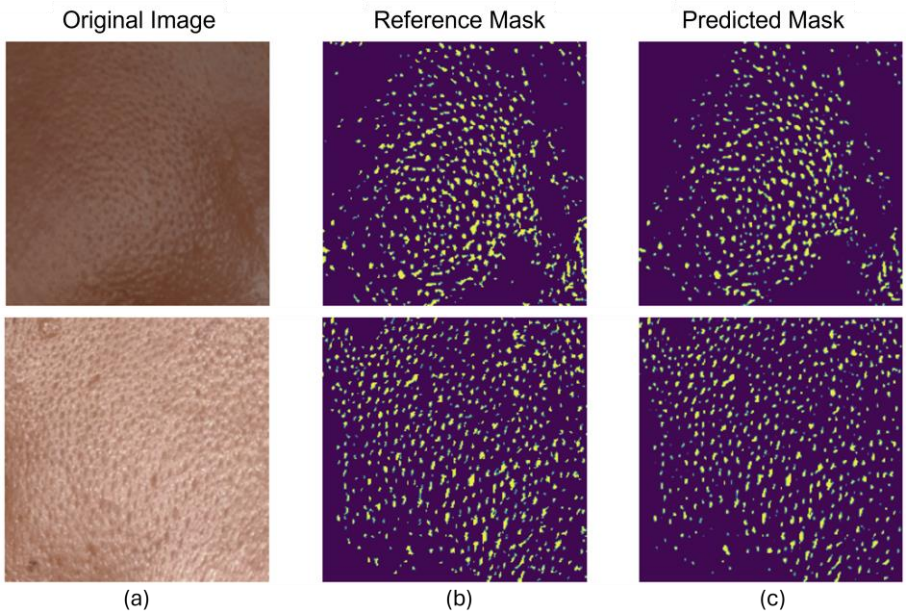

Figure 2. Pores detection by model performance: (a) Original input image; (b) Actual reference mask; (c) Predicted mask by the model.

3.2. Outcomes of the Pore Depth Classification method

Different parameters were obtained from the processed images. In this study, we focused on evaluating the pore surface and the pore distribution on the skin according to their depth, as these are the most remarkable parameters that can be extracted from a 3D device compared to what can be extracted from 2D images. Figure 3 presents the results derived from the processed image in Scheme 1. Out of 682 pores, which represent 58.52% of the total area, the results indicate that 50% of the pores are not very deep, while 36% have greater depth, making them more noticeable. These findings provide a quick visualization of how the pores affect the skin surface and offer precise numerical information on pore improvement after a treatment.

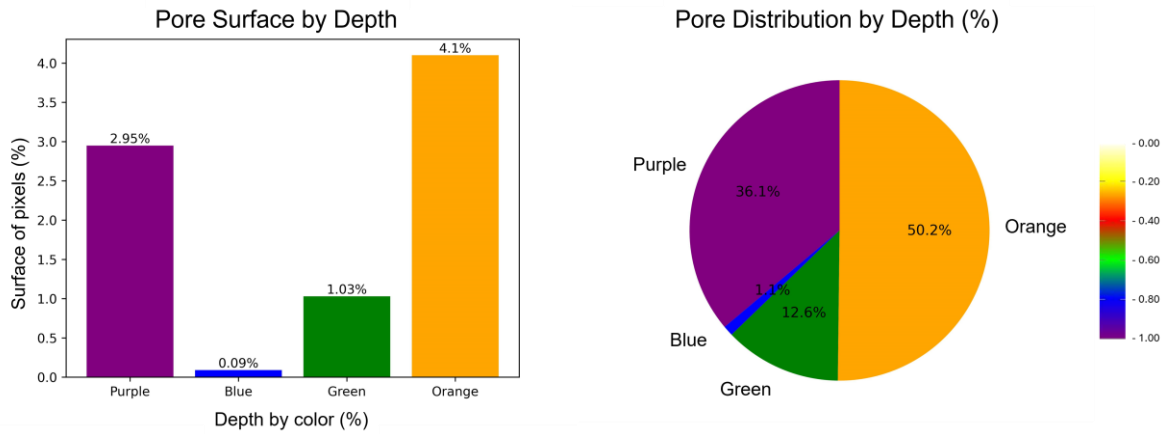

(a) (b)

Figure 3. Results of skin pore surface and distribution based on their depth: (a) Bar chart of total pore surface of the skin (%); (b) Pie chart of pores distribution on the skin (%).

3.3. Age-Related Pores from processed images.

After image processing, the age-related pores were analyzed. For each volunteer's cheek area image, we calculated several parameters including elongation ratio by dividing the major axis by the minor axis of the ellipse previously created. As shown in Figure 4, only the enlarged and elongated pores are displayed, providing a clear visual representation along with the precise values for each parameter. Table 1 presents the results obtained from image analysis. This detailed examination allows for a better understanding of how aging affects the pore morphology and its evolution over time.

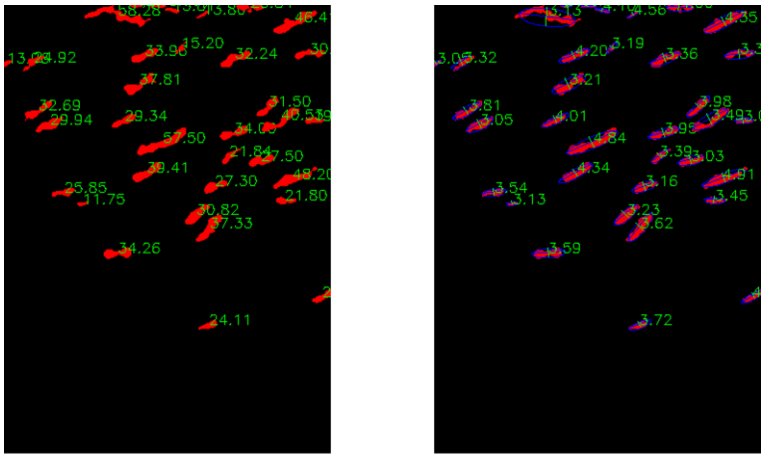

(a) (b)

Figure 4. Age-related pores image displaying from Scheme 2 image example after imaging processing: (a) Length values (px); (b) Elongation ratio values.

Table 1. Results of aged pore parameters from Scheme 2 image example after imaging processing.

Parameter	Value
Total pore number	35
Mean pore area (px^2)	149.80
Covered area (%)	3.29
Mean length (px)	29.49
Elongation ratio	3.70
Orange area (%)	9.90
Red area (%)	14.07
Yellow area (%)	12.39

4. Discussion

One of the key benefits of incorporating computer vision and AI in the laboratories is the acceleration of the workflow. The initial method developed leverages trained algorithms to detect the regions of interest where pores are more pronounced. By segmenting the cheek area, the system allows an automatic selection for displaying results without requiring manual delimitation each time. Additionally, the network generates smoother, masks of pores visibility and it is designed to evaluate facial images from different angles. As a next step, with the created mask, a quantification of different parameters of pore features will become a faster and easier process.

The second tool has demonstrated to be able to quantify several aspects of pores from 3D images. Using the scale color of highlighted pores that the software of the commercial device offers, our method provides numerical data about their attributes such as quantity and area, but also, it classifies them based on depth grading features, enhancing the image comprehension and delivering objective results.

The third application developed showed a good performance in subtracting age-related pores. By doing several steps with computer vision techniques, the resulting images are analyzed providing information such as number, area and elongation ratio. This approach allows a deeper analysis to evaluate how pores evolve in response to cosmetic treatments, surpassing the capabilities offered by software of commercial devices available until now.

The three methods have been developed for use with different types of images obtained by different devices, offering from rapid pore detection as an initial step to more specific analysis of parameters. In addition, these solutions can be easily integrated into a single analysis system adapted to the user's needs.

5. Conclusion

The evolution of the cosmetic industry has shifted from addressing traditional signs of aging to seeking to achieve a healthy aging appearance with completely flawless and impurity-free skin. Playing a key role in this goal, the minimization of pore visibility has become essential. To enhance the analysis of cosmetic treatments in improving pores, novel methods leveraging computer vision and artificial intelligence have been developed, representing a significant advancement in studying the pore features. These methods enable a quicker automatic identification of key facial regions, detailed pore detection, and comprehensive analysis using high-resolution 2D and 3D imaging. As a result, these new approaches provide a more accurate, objective, and detailed evaluation of pores, including in the context of age-related changes, opening the door to more effective evaluation of cosmetic treatments.

6. References

1. 2025 Beauty Trends Report. SPATE, 2024.
2. Zhou H, Xie H, Wu L, Song J, Ma Z, Zeng D, Wang X, Shi S, Qu Y, Luo Y, Meng X, Niu Y, Kan H, Cao J, Pernodet N. An artificial intelligence powered study of enlarged facial pore prevalence on one million Chinese from different age groups and its correlation with environmental factors. Skin Res Technol. 2024 Sep;30(9):e70025.
3. François G, Maudet A, McDaniel D, Giron F, Bazin R. Quantification of Facial Pores Using Image Analysis. J. Cosmet. Dermatol. 2009;22(9):457-463.
4. Google AI Edge. MediaPipe. [Internet]. [cited 2025 January]. Available from: https://github.com/google-ai-edge/mediapipe.
5. McKinley S, Levine M. Cubic spline interpolation. College of the Redwoods. 1988;45(1):1049-1060.
6. Chaudhari A. Review of Histogram Equalization Methods for Contrast Enhancement. CAE Proceedings on International Conference on Communication Technology. 2015 Sep;ICCT2015(5):20-24.
7. Dhanachandra N, Manglem K, Chanu YJ. Image segmentation using K-means clustering algorithm and subtractive clustering algorithm. Procedia Computer Science. 2015;54:764-771.
8. Computer Vision and Pattern Recognition. [Internet]. arXiv; [cited 2025 March]. Available from: https://arxiv.org/list/cs.CV/recent.
9. Kaiming H, Xiangyu Z, Shaoqing, Jian S. Deep residual learning for image recognition. Proceedings of the IEEE Conference on Computer Vision and Pattern Recognition (CVPR). 2016;770-778.
10. Rezatofighi H, Tsoi N, Gwak J, Sadeghian A, Reid I, Savarese S. Generalized inter-section over union. Proceedings of the IEEE Conference on Computer Vision and Pattern Recognition (CVPR). 2019;658-666.